DIMACS Technical Report 99-55
November 1999

Apparent Motion in Spatial Time-varying Data: A Variational Approach to Pointwise Tracking of Coherent Structures in Computational Fluid Dynamics

by

Vadim Mottl, Alexander Blinov
Tula State University
Lenin Ave. 92, 300600 Tula, Russia
mottl@atm.tsu.tula.ru
blinov@atm.tsu.tula.ru

Norman Zabusky
Department of Mechanical and Airspace Engineering
and CAIP Center, Rutgers University
P.O. Box 8018, Piscataway, NJ 08855
nzabusky@vizlab.rutgers.edu

Ilya Muchnik
DIMACS, Rutgers University
P.O. Box 8018, Piscataway, NJ 08855
muchnik@dimacs.rutgers.edu

DIMACS is a partnership of Rutgers University, Princeton University, AT&T Labs-Research, Bell Labs, Telcordia Technologies (formerly Bellcore) and NEC Research Institute.

DIMACS is an NSF Science and Technology Center, funded under contract STC–91–19999; and also receives support from the New Jersey Commission on Science and Technology.

ABSTRACT

By a massive time-varying data set is meant an experimentally acquired or mathematically simulated function of spatial coordinates and time which is to be analyzed with the purpose of studying behavior of the respective distributed dynamical system. We address here primarily problems of computational fluid dynamics that are concerned with the necessity to visualize and study overwhelming time-varying data sets generated by numerical unsteady simulations. Of a major interest is time tracking of persistent coherent structures of the fluid flow that use to arise, move in space for a time while, fade, and be replaced by new pattern building up from their remains. The spatial motion of persistent patterns in a time-varying data set is called here apparent motion because it does not coincide, in the general case, with mechanical motion of any physical particles. With the purpose of tracking coherent structures, it is proposed to evaluate the apparent motion in terms of apparent velocity of space points. The apparent velocity is to be estimated in the form of a time-varying vector field as result of processing the original time-varying data set or immediately in the course of numerical simulating the respective physical reality as solution of an additional system of partial differential equations. In both versions, we lean upon the variational approach to the analysis of massive data sets and estimate the vector field of apparent velocity as time-varying function that delivers the minimum value to a quadratic functional. In experiments with simulated two-dimensional time-varying spatial dynamics of the fluid's density and vorticity in shock wave interaction with an elliptical bubble, the estimated apparent velocity provided long-term pointwise tracking of persistent coherent structures.

Contents

1 Introduction

The necessity to analyze time-varying data sets inevitably arises in practice of scientific and engineering investigations when it is required to study behavior of distributed dynamical systems. The name of a time-varying data set $Y = (y(\mathbf{x}, t),\ \mathbf{x} \in \mathsf{X} \subset \mathsf{R}^n,\ t \in \mathsf{T})$ is applied to any collection of functions $y(\mathbf{x}, t) = \left(y^{(1)}(\mathbf{x}, t), \ldots, y^{(k)}(\mathbf{x}, t)\right)$ which is defined in space of a suitable dimensionality n and includes time t as one of its arguments. Data of such a kind show how constituents $y^{(k)}(\mathbf{x}, t)$ of the distributed state of the respective dynamical system change in space and time and are usually called $nD + 1$ time-varying data sets.

In particular, in fluid-dynamical studies, time-varying data sets are formed by constituents of the fluid flow's state at all the points of a fragment of one-, two- or three-dimensional space. For instance, density $\rho(\mathbf{x}, t)$, pressure $p(\mathbf{x}, t)$ and instantaneous velocity $\mathbf{u}(\mathbf{x}, t)$ form the basic set of state variables for ideal compressible fluid. It is just these variables that are bound by the systems of Euler and Navier-Stokes partial differential equations for, respectively, the inviscid and viscid case. However, it is often preferable to study time-varying data sets formed by other characteristics of the fluid flow, namely, some functions of the basic state variables. For instance, vorticity which is defined as rotation of the vector field formed by instantaneous velocity $\omega(\mathbf{x}, t) = \mathrm{Rot}\,(\mathbf{u}(\mathbf{x}, t))$ is useful for studying vortical structures in a fluid flow. Vorticity forms a time-varying vector field in the three-dimensional space, but in the two-dimensional case $\mathbf{u}(\mathbf{x}, t) = (u_1(x_1, x_2, t), u_2(x_1, x_2, t))$ this characteristic is a scalar variable $\omega(x_1, x_2, t) = \partial u_2/\partial x_1 - \partial u_1/\partial x_2$ whose magnitude and sign indicate the intensity and direction of rotation.

The time-varying data set subject to an analysis can be acquired experimentally or obtained from a mathematical model as result of numerical simulation. In both cases, a data set can be represented in computer only in the discrete form as an array defined by discrete values of the spatial arguments and time varied with preset steps. Nevertheless, an exhaustive mathematical model determines, at least, theoretically, the functions of continuous arguments which are the generic form of a time-varying data set. A data set in the form of a finite collection of values at discrete points of a lattice is result of sampling a hidden time-varying function in continuous space-time.

As example of a simulated $2D + 1$ time-varying data set, Fig. 1 shows a series of density $\rho(x_1, x_2, t)$ and vorticity images $\omega(x_1, x_2, t)$ that represent selected phases of the interaction of a shock wave with an elliptical bubble of gas heavier than the ambient medium. The data set is obtained as solution of the system of Euler equations with respective initial and boundary conditions.

In comparison with massive data sets of general kind, a substantial specificity of a time-varying data set consists in that it is meant to describe time evolution of a distributed spatial reality through all the successive time moments, in other words, to be carrier of information on some kind of motion in space. This fact places some special demands on the algorithms of data analysis, the major of which is the necessity to track changes in the position and properties of relatively persistent single objects constituting a time-varying image.

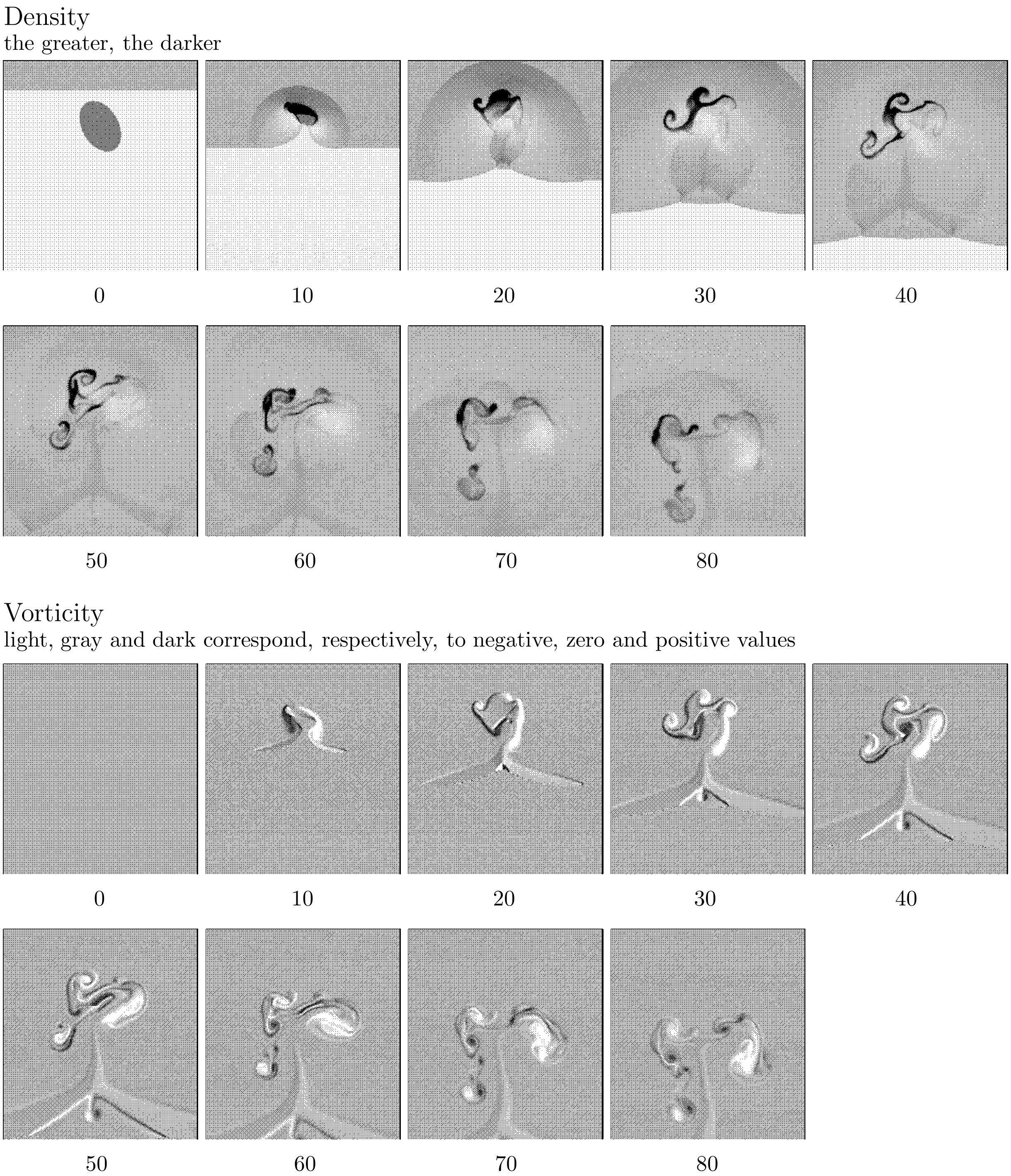

Figure 1: Selected phases of simulated shock wave interaction with an elliptical bubble of gas.

The principle of extracting and tracking objects of interest in time-varying data which was proposed in the previous research [1, 2] is based on the definition of an object at a discrete time moment $t_j = j\Delta t$ as a connected region in the space where the scalar function under examination takes values between two thresholds $a \leq y(\mathbf{x}, t_j) \leq b$ given by the researcher. In the general case, there are several connected areas of such a kind at each t_j, let them be denoted by symbols $O_j^1, \ldots, O_j^{m_j}$, and the number of them m_j may be different at different time moments. The problem of tracking objects of interest is set in [1, 2] as that of establishing a pairwise correspondence between objects at every two adjacent time moments t_j and t_{j+1} in accordance with the criterion of the maximum intersection area. There are five possible kinds of correspondence. An object at t_j is said to dissipate, be continued, or split, if it is associated with, respectively, no, one, or several objects at t_{j+1}. Several objects at t_j merge into one, if they correspond to the same object at t_{j+1}. Finally, an object at t_{j+1} is proclaimed to be created, if no object at t_j is associated with it.

Such a principle of tracking should be called isosurface-oriented, because the boundaries of objects being tracked in time are formed by isosurfaces of the function in accordance with the preset pair of thresholds. However, with other thresholds other objects will be extracted, and the operation of tracking must be done anew.

On the basis of the same isosurface-oriented principle, we propose here an improved tracking technique based on the idea to follow in time not the entire regions cut out by that or other pair of thresholds but all the single points of the space. The tracking problem is set as that of finding a sufficiently smooth vector function of spatial shifts $Z = (z(\mathbf{x}, t),\, \mathbf{x} \in \mathsf{X},\, t \in \mathsf{T})$ that, for each space point $\mathbf{x} \in \mathsf{X} \subset \mathsf{R}^n$ at a time moment t_j, indicates its best match $\mathbf{x} + \mathbf{z}(\mathbf{x}, t_j) \in \mathsf{R}^n$ at the next time moment t_{j+1}. We keep here within the bounds of the so called variational approach to the analysis of ordered data sets [3, 4], and in accordance with this concept we understand the desired result of tracking as function

$$\hat{Z} = (\hat{\mathbf{z}}(\mathbf{x}, t),\, \mathbf{x} \in \mathsf{X},\, t \in \mathsf{T}) = \arg\min_{Z} J(Z, Y) \tag{1}$$

that minimizes a functional $J(Z, Y)$ built as sum of squared differences $[y(\mathbf{x}, t) - y\left(\mathbf{x} + \mathbf{z}(\mathbf{x}, t),\, t_{j+1}\right)]^2$ over all the pairs $(\mathbf{x} \in \mathsf{X},\, t_j \in \mathsf{T})$ plus some penalty imposed on unsmoothness of Y.

So, for any pair of thresholds, the resulting vector function $Z = (\mathbf{z}(\mathbf{x}, t),\, \mathbf{x} \in \mathsf{X},\, t \in \mathsf{T})$ is meant to map each point inside a connected region $\mathbf{x} \in \{\mathbf{x}' :\, a \leq y(\mathbf{x}', t_j) \leq b\}$ into a point inside the corresponding region $\mathbf{x} + \mathbf{z}(\mathbf{x}, t_j) \in \{\mathbf{x}' :\, a \leq y(\mathbf{x}', t_{j+1}) \leq b\}$, and vice versa, an outside point at t_j should match a point outside the region at the next time moment t_{j+1}. In this sense, the result of tracking remains the same, but it is enough to apply the improved tracking operation only once, and it will establish the desired relationship between regions of interest for all the threshold values.

In this work, we propose a tracking algorithm which is an approximate discrete realization of such a principle of object tracking in time-varying data sets for the case of two-dimensional space $\mathbf{x} = (x_1, x_2)$. But the structure of the algorithm will remain the same for the three-dimensional space and, if required, for spaces of greater dimensionality.

With $\Delta t = t_{j+1} - t_j \to 0$, the vector shifts will infinitesimally diminish, and, instead of full shifts, normalized vectors should be considered $\mathbf{v}(\mathbf{x}, t)/\Delta t$. In the limiting case, the vectors $\mathbf{v}(\mathbf{x}, t)$ have the sense of instantaneous local velocities, but the kind of motion they evaluate is no physical one. In this work, the motion resulting from the relative stability of patterns in a time-varying data set is called the apparent motion. It is shown in Section ?, that for infinitesimally small time steps the condition (1) leads to a system of partial differential equations which the optimal vector function $V = (\mathbf{v}(\mathbf{x}, t),\, \mathbf{x} \in \mathsf{X},\, t \in \mathsf{T})$ has to satisfy.

The structure of the work is as follows. In Section 2, the generalized structure of a time-varying data set is considered and main denotations are introduced. The notion of apparent motion is preliminarily discussed in Section ?. The algorithmical principles of apparent motion evaluation in time-varying data sets on discrete time axis are proposed in Section ?. Some experimental results on the evaluation of apparent motion and time tracking of coherent structures in density and vorticity images of simulated shock wave interaction with an elliptical bubble of gas are presented in Section ?. Finally, in Section ?, the problem of apparent velocity evaluation is discussed as that of solving a system of partial differential equations immediately in the process of simulating the physical process under investigation.

2 Structure of a time-varying data set

Under a time-varying data set, we understand here any real-valued scalar $y(\mathbf{x}, t)$ or vector function $y(\mathbf{x}, t) = \left(y^{(1)}(\mathbf{x}, t), \ldots, y^{(k)}(\mathbf{x}, t)\right)$ which is defined in a rectangular region of the vector space $\mathbf{x} = (x_1, \ldots, x_n) \in \mathsf{X}$, $x_i^{\min} \le x_i \le x_i^{\max}$, and includes time t as one of its arguments. A natural interpretation of a time-varying data set is the view on it as time evolution $t^{\min} \le t \le t^{\max}$ of the respective function defined in space, as a rule, the one-dimensional $\mathbf{x} = x \in \mathsf{R}$, two-dimensional $\mathbf{x} = (x_1, x_2) \in \mathsf{R}^2$, or three-dimensional one $\mathbf{x} = (x_1, x_2, x_3) \in \mathsf{R}^3$.

Such a structure of a data set is the natural desire in many scientific and engineering investigations. In this work, we address primarily the time-varying data sets related to problems of fluid dynamics.

In the cases when immediate physical experiments are possible and their results lend themselves to instrumental documentation, the time-varying function of interest $y(\mathbf{x}, t) = y(x_1, \ldots, x_n, t)$ can be registered experimentally only in the form of a data array defined by discrete values of the spatial arguments $\mathbf{x_i} = (x_{1,i_1} = i_1 \Delta x, \ldots, x_{n,i_n} = i_n \Delta x)$ and time $t_j = j\Delta t$ varied with preset steps Δx and Δt:

$$\begin{aligned} &Y = (y(\mathbf{x_i}, t_j) = y_{\mathbf{i},j},\ \mathbf{i} \in \mathsf{N},\ j \in \mathsf{K}), \\ &\mathsf{N} = \{\mathbf{i} = (i_1, \ldots, i_n):\ i_1 = 1, \ldots, N_1,\ \ldots,\ i_n = 1, \ldots, N_n)\}, \\ &\mathsf{K} = \{j:\ j = 1, \ldots, K\}. \end{aligned} \tag{2}$$

We shall use the denotation $Y_j = (y_{\mathbf{i},j},\ \mathbf{i} \in \mathsf{N},\ j = \text{const})$ for single time slices within the entire time-varying data set.

If an exhaustive mathematical model of the process under investigation is available, usually, in the form of a system of partial differential equations, the time-varying function satisfying the model can be obtained as result of a computational experiment instead of an immediate physical one. Despite the fact that, just as in the case of physical experiments, a numerical solution of the respective computational problem can be obtained only in the discrete form like (2), the model determines, at least, theoretically, the function of continuous arguments

$$\begin{aligned}&Y = (y(\mathbf{x}, t),\, \mathbf{x} \in \mathsf{X},\, t \in \mathsf{T})\,,\\ &\mathsf{X} = \left\{\mathbf{x} = (x_1, \ldots, x_n) \in \mathsf{R}^n :\ x_i^{\min} \le x_i \le x_i^{\max},\, i = 1, \ldots, n\right\},\\ &\mathsf{T} = \left\{t \in \mathsf{R} :\ t^{\min} \le t \le t^{\max}\right\}.\end{aligned} \tag{3}$$

Single time slices of the entire function will be denoted hereafter as $Y(t) = (y(\mathbf{x}, t)$, $\mathbf{x} \in \mathsf{X}$, $t = \text{const})$.

What is especially important for the further consideration is the fact that each element of a time slice, let it be element of a continuous $\mathbf{x} \in \mathsf{X} \subset \mathsf{R}^n$ or discrete data set $\mathbf{x_i}$, $\mathbf{i} \in \mathsf{N}$, is naturally associated with its immediate vicinity in the space. In the continuous case, the "immediate vicinity" is infinitesimally small and understood as the "set" accessible from $\mathbf{x} = (x_1, \ldots, x_n)$ by infinitesimally small increments in the coordinates $dx_1, \ldots, dx_n$. But for discrete data arrays, we have to take care of giving a definition to the finite set of spatial neighbors that we want to understand as the immediate vicinity of an element $\mathbf{x_i}$. For a single time slice, it is convenient to express the neighborhood relation on the set of discrete elements of the space interval under consideration $\mathbf{i} \in \mathsf{N}$ in the form of an undirected graph G_j which remains the same for all the discrete time moments and is understood as the set of neighboring pairs of elements $G_j \in \mathsf{N} \times \mathsf{N}$. In this work, we restrict our concern to $2D+1$ time-varying data sets, in which case a time slice is represented in an interval of the two-dimensional space. The natural neighborhood graph G_j for elements of a two-dimensional space will be two-dimensional rectangular lattice (Fig. 2,a).

Furthermore, the like elements $\mathbf{i} = (i_1, \ldots, i_n)$ of any two adjacent time slices Y_j and Y_{j+1} are neighbors along the time axis in the time-varying data set (2) as a whole. We shall express this neighborhood relation as a graph $G \in \mathsf{N} \times \mathsf{N} \times \mathsf{T}$ defined on the full set of variables. In case of $2D+1$ data sets we focus on in this work, the simplest form of the full neighborhood graph is regular three-dimensional lattice (Fig. 2,b).

3 Actual and apparent motion in fluid-dynamical time-varying data sets

Any model that determines a time-varying function in a continuous domain $\mathsf{X} \in \mathsf{T}$ (3) in the form of a system of partial differential equations is inevitably the model of a dynamic system in which the instantaneous time slice $Y(t)$ plays the role of the state variable taking values from the respective state space $\mathcal{Y}$. This means that the model defines the variation

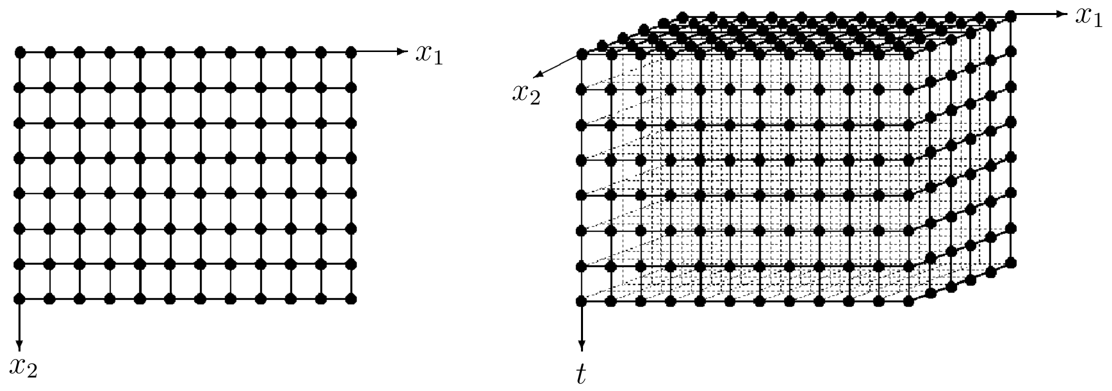

(a) (b)

Figure 2: Neighborhood graphs for elements of a two-dimensional data set (a) and the respective time-varying set (b).

$Y(t+dt) \in \mathcal{Y}$ for any current state $Y(t) \in \mathcal{Y}$ in the form of an equation $\mathcal{F}\left(Y(t),\, Y(t+dt)\right) = 0$. Thus, once the initial state $Y(t_0) \in \mathcal{Y}$ is given, the model completely determines all the future states $Y(t)$, $t > t_0$.

If a discrete data set (2) is meant as result of a plain quantization of a time-varying function (3) described by a state-space model, the resulting finite representation $Y_j = Y(t_j)$ of $Y(t)$ will, in the general case, no longer possess the properties of a state variable relative to this model, so that the existence of a recurrent model $\mathcal{F}'\left(Y_j, Y_{j+1}\right) = 0$ will be rather an exclusion than the rule.

So, from the viewpoint of the physical laws regulating the behavior of the reality under investigation and having the form of a system of partial differential equations, the continuous form (3) is the generic one, whereas the discrete form (2) is meant as a rough representation of it. In this work, we shall pay attention to both of these forms of representing time-varying data.

For instance, in the models of fluid dynamics written in the form of the Euler equations for inviscid compressible fluid

$$\begin{cases} \dfrac{\partial}{\partial t}\rho(\mathbf{x},t) + \mathrm{Tr}\left[\nabla_{\mathbf{x}}\left(\mathbf{u}(\mathbf{x},t)\rho(\mathbf{x},t)\right)\right] = 0, \\ \dfrac{\partial}{\partial t}\left(\mathbf{u}(\mathbf{x},t)\rho(\mathbf{x},t)\right) + \left[\nabla_{\mathbf{x}}\left(\mathbf{u}(\mathbf{x},t)\rho(\mathbf{x},t)\right)\right]\mathbf{u}(\mathbf{x},t) + \nabla_{\mathbf{x}} p(\mathbf{x},t) = \mathbf{0}, \\ \dfrac{\partial}{\partial t}\left(E(\mathbf{x},t)\rho(\mathbf{x},t)\right) + \sum\limits_{i=1}^{n}\dfrac{\partial}{\partial x_i}\left(u_i(\mathbf{x},t)E(\mathbf{x},t)\rho(\mathbf{x},t)\right) + \mathrm{Tr}\left[\nabla_{\mathbf{x}}\left(\mathbf{u}(\mathbf{x},t)p(\mathbf{x},t)\right)\right] = 0, \end{cases} \tag{4}$$

where $\mathrm{Tr}\mathbf{A} = \sum_{i=1}^{n} a_{ij}$ is track of matrix $\mathbf{A} = \{a_{ij},\, i,j = 1,\ldots,n\}$, the state variable consists of the vector velocity $\mathbf{u}(\mathbf{x},t) = (u_1(\mathbf{x},t), u_2(\mathbf{x},t), u_3(\mathbf{x},t))$, mass density $\rho(\mathbf{x},t)$ and pressure $p(\mathbf{x},t)$, that are considered jointly as instantaneous functions over the space domain being examined $Y(t) = (\mathbf{u}(\mathbf{x},t), \rho(\mathbf{x},t), p(\mathbf{x},t); \mathbf{x} \in \mathsf{X})$. In this equation system $E(\mathbf{x},t) = \frac{1}{2}\mathbf{u}^T(\mathbf{x},t)\mathbf{u}(\mathbf{x},t) + \frac{1}{\gamma-1}\frac{p(\mathbf{x},t)}{\rho(\mathbf{x},t)}$ is function of the state variables called specific energy, and γ is ratio of specific heats.

In the language of dynamic systems theory, all the kinds of changes occurring in $Y(t)$ with time in accordance with the respective model are called systemic motion. In particular, the usual mechanical motion of some physical objects included in a system is one of the possible kinds of changes in its state which are embraced by this generalized term.

As to the models of fluid dynamics, only one of the aspects of the generalized systemic motion in $Y(t)$, namely, that expressed by the instantaneous velocity $\mathbf{u}(\mathbf{x},t)$, has the sense of the actual mechanical motion of elementary particles of fluid in space. This motion can be shown explicitly in the Lagrangian formulation as the family of particle trajectories $\mathbf{x}(\mathbf{x}_0,t_0,t)$, the so-called stream-lines, that result from the differential equation $\frac{\partial}{\partial t}\mathbf{x}(\mathbf{x}_0,t_0,t) = \mathbf{u}(\mathbf{x},t)$ with the initial conditions $\mathbf{x}(\mathbf{x}_0,t_0,t) = \mathbf{x}_0 \in \mathsf{X}$.

The changing values of the state constituents themselves at any fixed point of the space $(\mathbf{u}(\mathbf{x},t), \rho(\mathbf{x},t), p(\mathbf{x},t); \mathbf{x} = \text{const})$ should be considered as other kinds of systemic motion, which cannot be reduced to changes in spatial positions of any physical objects.

However, if one looks at the succession of time slices of a time-varying function as pictures forming a kind of movies $\{Y(t), Y(t+\Delta t), Y(t+2\Delta t), \ldots\}$ with a not too large time step, let it be density, pressure or vector velocity, it will be easy to mark that, as a rule, the form of the functions shows a high degree of stability in time within quite large space regions called coherent structures. However, this relative persistence of coherent structures is evident only if the respective regions are considered as moving in space, namely, translating and rotating. The existing means of visiometrics [5] are aimed at pictorial representation of just this kind of motion which is an intrinsic property of the process under investigation.

The approach to studying processes of fluid dynamics based on extraction and tracking quasi-stable patterns, the so-called coherent structures, is gaining an increasing adoption [6]. Enhanced by the means of visiometrics, this methodology provides peak insights for discovery of hardly observable phenomena in fluid behavior.

The motion of persistent patterns over space is no mechanical one and does not coincide, in the general case, with that of elementary fluid particles. Nevertheless, it has much in common with the usual motion in the sense that it is possible to indicate the identical points in subsequent functions and track their routes in space. In contrast to the actual motion, it is not always possible to perform such an identification over a long time interval. Sufficiently clear patterns which are the only carriers of space points identity use to arise, exist a time while, and decay. But, as a rule, new patterns build up from the remains of the fading ones. In general, it is practically always possible to track the points of a pattern over a marked time and, hence, speak about the instantaneous direction and speed of their motion.

In this work, we propose to call the motion resulting from the relative persistence of patterns in a time-varying data set the apparent motion.

The apparent motion of a space point is meant to be expressed by its trajectory which should be called, by analogy to the actual motion, the apparent streamline. However, this term leads to the necessity to accept some more definite assumptions on the properties of the apparent motion and eliminate the existing ambiguity. May the apparent streamlines intersect in space-time? May they merge? May they split? If they may or not may do this, what is the expected form of the apparent streamlines, i.e. the dynamics of the sough-for apparent motion? The answers to these questions cannot be given without taking into account the working hypotheses on the reality under investigation posed by the researcher.

Hence, there is a fundamental difference in time-varying data sets related to fluid dynamics between the actual motion of fluid particles and the apparent motion. Whereas the actual motion is completely determined by the respective system of differential equations, for the evaluation of the apparent one some additional assumptions should be chosen in accordance with the researcher's view of the hidden phenomenon being studied.

In this work, we restrict our concern to the assumption that apparent streamlines do not intersect and, hence, only one streamline can be associated with a point $(\mathbf{x}, t)$ of the space-time. If it is done, the direction and speed of the apparent motion is determined at this point in the form of an apparent velocity vector.

4 Evaluation of apparent motion in discrete time-varying data sets

The problem of the isosurface-based tracking, as it is preliminarily formulated in the Intriduction, is analogous to a standard problem of image analysis known under the name of image matching. In the matching problem, a pair of images of the same size is analyzed, for instance, two human portraits or a stereo pair of photographs of the same object taken from two slightly different directions (Fig. 3). Each of the images forming a pair, let it conventionally be the left $Y^l = \left(y^l_{i_1,i_2},\, (i_1,i_2)\in \mathsf{N}\right)$ and the right image $Y^r = \left(y^r_{i_1,i_2},\, (i_1,i_2)\in \mathsf{N}\right)$, is a two-dimensional array of darkness values at the elements of a rectangular pixel grid $\mathsf{N} = \{(i_1,i_2);\, i_1 = 1,\dots,N_1,\, \dots\, ,\, i_2 = 1,\dots,N_2\}$, and the pair as a whole can be considered as a two-component array. It is required to establish a correspondence in the two images between the pairs of points which could be treated as identical. The result of such an operation is usually represented in the form of the so-called disparity map $Z = \left(\mathbf{z}_{i_1,i_2} = (z^{(1)}_{i_1,i_2}, z^{(2)}_{i_1,i_2}),\, (i_1,i_2)\in\mathsf{N}\right)$ that, for each point (i_1,i_2) of the one of the images (for instance, the left one taken as reference image) determines the vector $\mathbf{z}_{i_1,i_2} = (z^{(1)}_{i_1,i_2}, z^{(2)}_{i_1,i_2})$ indicating the spatial shift between (i_1,i_2) and its match $(i'_1,i'_2) = \left(i_1 + z^{(1)}_{i_1,i_2},\, i_2 + z^{(2)}_{i_1,i_2}\right)$ in the second (search) image as it is shown in Fig. 3.

Practically the same is required in the problem of tracking, where the role of a pair of images subject to the matching operation is played by the pair of adjacent time slices $Y_j = (y_{\mathbf{i},j},\, \mathbf{i}\in\mathsf{N})$ and $Y_{j+1} = (y_{\mathbf{i},j+1},\, \mathbf{i}\in\mathsf{N})$.

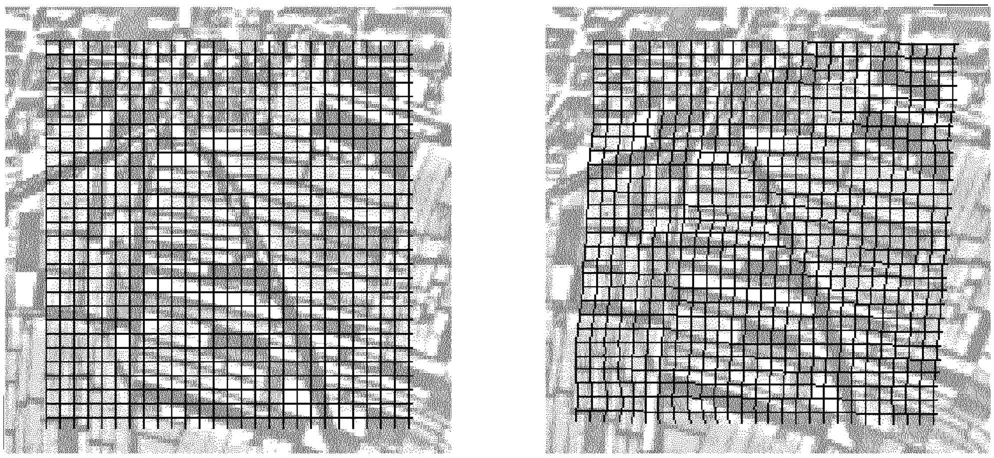

Figure 3: Disparity map of a stereo pair of satellite photographs.

The dimension of the space is not critical for the structure of the matching procedure, it may be one-dimensional $\mathbf{z}_i = z_i$, two-dimensional $\mathbf{z}_{i_1,i_2} = \left(z^{(1)}_{i_1,i_2}, z^{(2)}_{i_1,i_2}\right)$, three-dimensional $\mathbf{z}_{i_1,i_2,i_3} = \left(z^{(1)}_{i_1,i_2}, z^{(2)}_{i_1,i_2}, z^{(3)}_{i_1,i_2}\right)$ or more-dimensional space, but we shall assume, within the bounds of this work, that a $2D+1$ time-varying data set is to be analyzed.

In accordance with the isosurface-based principle of tracking, or, more appropriately, the isoline-based one in the case of the two-dimensional space, it is required to find, for each pair of time slices Y_j and Y_{j+1}, a disparity map

$$Z_j = \left(\mathbf{z}_{\mathbf{i},j} = (z^{(1)}_{\mathbf{i},j}, z^{(2)}_{\mathbf{i},j}),\ \mathbf{i} \in \mathsf{N}\right),$$
$$\mathsf{N} = \{\mathbf{i} = (i_1, i_2) :\ i_1 = 1, \dots, N_1,\ i_2 = 1, \dots, N_2\}$$

that should satisfy the condition $y_{\mathbf{i},j} = y_{\mathbf{i}+\mathbf{z}_{\mathbf{i},j},j}$. But such a requirement is ambiguous, because there are many disparity vectors $\mathbf{z}_{\mathbf{i},j}$ that point at the same isoline in Y_{j+1}. To avoid this ambiguity, it appears reasonable to replace the rigid condition $y_{\mathbf{i},j} = y_{\mathbf{i}+\mathbf{z}_{\mathbf{i},j},j}$ by a milder one

$$\psi_{\mathbf{i},j}(\mathbf{z}_{\mathbf{i},j}|Y_j, Y_{j+1}) = \left(y_{\mathbf{i},j} - y_{\mathbf{i}+\mathbf{z}_{\mathbf{i},j},j}\right)^2 \rightarrow \min \tag{5}$$

with some additional smoothness constraints posed on the sought-for disparity map Z_j with the purpose to mutually coordinate its elements.

It is pertinent to call the disparity map Z_j associated with two adjacent slices of a time-varying data set on the axis of discrete time the instantaneous apparent motion map, because each of the vectors $\mathbf{z}_{\mathbf{i},j}$ shows the change in the position $\mathbf{i}' = \mathbf{i} + \mathbf{z}_{\mathbf{i},j}$ of the respective element $\mathbf{i}$ of the precedent picture Y_j over a single time step $t_{j+1} = t_j + \Delta t$ having led to the next picture Y_{j+1}.

If we abstract from the discrete nature of the pixel grid N and allow apparent motion vectors to take real values with the respective interpolation, the sought-for apparent motion map $Z_j = (\mathbf{z}_{\mathbf{i},j} = \mathbf{z}(\mathbf{x}_\mathbf{i}, t_j),\ \mathbf{i} \in \mathsf{N})$ can be considered as forming a mapping

$\mathbf{x}' = \mathbf{x} + \mathbf{z}(\mathbf{x}, t_j)$ of the space R^2 into itself. The variational approach to apparent motion evaluation is underlain by the idea of representing the distinction between two adjacent pictures $Y_j = (y_{\mathbf{i},j} = y(\mathbf{x}_\mathbf{i}, t_j),\ \mathbf{i} \in \mathsf{N})$ and $Y_{j+1} = (y_{\mathbf{i},j+1} = y(\mathbf{x}_\mathbf{i}, t_{j+1}),\ \mathbf{i} \in \mathsf{N})$ as sum $y\left(\mathbf{x} + \mathbf{z}(\mathbf{x}, t_j),\ t_{j+1}\right) = y(\mathbf{x}, t_j) + \xi_j(\mathbf{x})$ and by the intent to choose a sufficiently smooth one-to-one mapping $\mathbf{x} + \mathbf{z}(\mathbf{x}, t_j)$ so that the norm of the remainder $\xi_j(\mathbf{x})$ would be as small as possible. The criterion of the respective optimization problem has the following structure.

The data-dependent functions $\psi_{\mathbf{i},j}(\mathbf{z}_{\mathbf{i},j}|Y_j, Y_{j+1})$ are associated with single variables $\mathbf{z}_{\mathbf{i},j} \in \mathsf{Z} = \mathsf{R}^2$, i.e. with the nodes of the full neighborhood graph G, as well as with those of the subgraphs G_j each of which is related to a single time slice, therefore, we shall call them the node functions. Each of these functions expresses a preliminary fuzzy judgment on the value of the respective hidden variable $\mathbf{z}_{\mathbf{i},j} \in \mathsf{Z}$ and takes the greater value the more evident is the contradiction between, on the one hand, the hypothesis that $\mathbf{i}' = \mathbf{i} + \mathbf{z}_{\mathbf{i},j}$ is just the "correct" local shift we are seeking and, on the other hand, the difference between the values $y_{\mathbf{i},j}$ and $y_{\mathbf{i}+\mathbf{z}_{\mathbf{i},j},j+1}$ in the adjacent time slices. Let the functions $\psi_{\mathbf{i},j}(\mathbf{z}_{\mathbf{i},j}|Y_j, Y_{j+1})$ be called node functions, because each of them is associated with a node of the neighborhood graph on the set of data array elements (Fig. 2,b).

The smoothness constraints can be expressed in local terms as appropriate penalty functions $\gamma_{\mathbf{i}',\mathbf{i}'',j}(\mathbf{z}_{\mathbf{i}',j}, \mathbf{z}_{\mathbf{i}'',j})$ and $\gamma_{\mathbf{i},j,j+1}(\mathbf{z}_{\mathbf{i},j}, \mathbf{z}_{\mathbf{i},j+1})$ that should be defined at each pair of neighboring elements of the time-varying data array $(\mathbf{i}', \mathbf{i}'', j)$, $(\mathbf{i}, j, j+1) \in G \subset \mathsf{N} \times \mathsf{N} \times \mathsf{K}$ (Fig. 2,b) and take the greater values the greater is the discrepancy between the neighboring values, respectively, $\mathbf{z}_{\mathbf{i}',j}$ and $\mathbf{z}_{\mathbf{i}'',j}$ or $\mathbf{z}_{\mathbf{i},j}$ and $\mathbf{z}_{\mathbf{i},j+1}$, so that $\gamma_{\mathbf{i}',\mathbf{i}'',j}(\mathbf{z}_{\mathbf{i}',j}, \mathbf{z}_{\mathbf{i}'',j}) = 0$ if $\mathbf{z}_{\mathbf{i}',j} = \mathbf{z}_{\mathbf{i}'',j}$ and $\gamma_{\mathbf{i},j,j+1}(\mathbf{z}_{\mathbf{i},j}, \mathbf{z}_{\mathbf{i},j+1}) = 0$ if $\mathbf{z}_{\mathbf{i},j} = \mathbf{z}_{\mathbf{i},j+1}$. These functions will be referred to as edge functions, since each of them is associated with an edge of the neighborhood graphs G_j and G (Fig. 2).

If the pairs of adjacent time slices $Y_j = (y_{\mathbf{i},j},\ \mathbf{i} \in \mathsf{N})$ and $Y_{j+1} = (y_{\mathbf{i},j+1},\ \mathbf{i} \in \mathsf{N})$ are considered separately of the others, the decision on each secondary array as a whole $Z_j = (\mathbf{z}_{\mathbf{i},j},\ \mathbf{i} \in \mathsf{N})$ should be sought for as a compromise between the mutually contradictory requirements to minimize both node and edge functions. It is natural to take the sum

$$J_j(Z_j, Y_j, Y_{j+1}) = \sum_{\mathbf{i}\in\mathsf{N}} \psi_{\mathbf{i},j}(\mathbf{z}_{\mathbf{i},j}|Y_j, Y_{j+1}) + \sum_{(\mathbf{i}',\mathbf{i}'')\in G} \gamma_{\mathbf{i}',\mathbf{i}'',j}(\mathbf{z}_{\mathbf{i}',j}, \mathbf{z}_{\mathbf{i}'',j}) \tag{6}$$

as a combined criterion of decision making for an isolated pair of time slices:

$$\hat{Z}_j(Y_j, Y_{j+1}) = \arg\min_{\mathbf{z}_{\mathbf{i},j}\in\mathsf{Z}} J_j(Z_j, Y_j, Y_{j+1}). \tag{7}$$

The succession of space shift arrays $\hat{Z}_j(Y_j, Y_{j+1})$, $j = 1, \dots, K$, is the final result of tracking if no smoothness constraints are imposed upon the local shifts at the same space point at two adjacent time moments, i.e. if $\gamma_{\mathbf{i},j,j+1}(\mathbf{z}_{\mathbf{i},j}, \mathbf{z}_{\mathbf{i},j+1}) \equiv 0$. Otherwise, the full array of space shifts between all the adjacent time slices is to be found as solution of a joint optimization problem

$$J(Z, Y) = \sum_{j=1}^{K} \left\{ \sum_{\mathbf{i}\in\mathsf{N}} \psi_{\mathbf{i},j}(\mathbf{z}_{\mathbf{i},j}|Y_j, Y_{j+1}) + \sum_{(\mathbf{i}',\mathbf{i}'')\in G} \gamma_{\mathbf{i}',\mathbf{i}'',j}(\mathbf{z}_{\mathbf{i}',j}, \mathbf{z}_{\mathbf{i}'',j}) \right\} + \sum_{j=1}^{K-1} \gamma_{\mathbf{i},j,j+1}(\mathbf{z}_{\mathbf{i},j}, \mathbf{z}_{\mathbf{i},j+1}), \tag{8}$$

$$\hat{Z}(Y) = \arg \min_{\mathbf{z}_{\mathbf{i},j} \in \mathsf{Z}} J(Z, Y). \tag{9}$$

As we see, the criterion to be minimized is in both cases a sum of items each of which is function of only one or two variables. The arguments of the criterion along with data-dependent functions are associated with elements of the data array, i.e. with nodes of the neighborhood graphs G_j and G (node functions), whereas the functions of two arguments are assigned to edges of the graphs (edge functions). We shall call an objective function of such a kind (6) or (8) to be separable, pairs of its variables occurring in summands $\gamma_{\mathbf{i}',\mathbf{i}'',j}(\mathbf{z}_{\mathbf{i}',j}, \mathbf{z}_{\mathbf{i}'',j})$ and $\gamma_{\mathbf{i},j,j+1}(\mathbf{z}_{\mathbf{i},j}, \mathbf{z}_{\mathbf{i},j+1})$ to be adjacent, and the graph G_j or G, that determines the structure of the respective function, its adjacency or supporting graph [4]. The number of variables in a separable objective function is equal to the number of nodes in its supporting graph, i.e. the number of elements in the respective data array. Namely, in the case of $2D+1$ time-varying data sets, $|\mathsf{N}| = N_1 N_2$ in (6) and $|\mathsf{N} \times \mathsf{K}| = N_1 N_2 K$ in (8).

As noted above, it is convenient to allow the spatial shift $\mathbf{z}_{\mathbf{i},j}$ which is originally conceived as integer to take values from the two-dimensional real space $\mathsf{Z} = \mathsf{R}^2$, and permit, thereby, inter-pixel interpolation in the discrete image grid N [4]. If the time step $\Delta t = t_{j+1} - t_j$ is small, and $y(\mathbf{x}, t)$ is a smooth function both in space and time, the expected space shift will be also small. In this case, the function $y_{\mathbf{i}+\mathbf{z}_{\mathbf{i},j},j} = y\big((\mathbf{i} + \mathbf{z}_{\mathbf{i},j})\Delta x,\, (j+1)\Delta t\big)$ can be approximately considered as linear function of the continuous shift

$$y\big((\mathbf{i} + \mathbf{z}_{\mathbf{i},j})\Delta x,\, (j+1)\Delta t\big) \cong y_{\mathbf{i},j} + \big[\nabla_{\mathbf{x}} y\big(\mathbf{i}\Delta x,\, (j+1)\Delta t\big)\big]^T \mathbf{z}_{\mathbf{i},j} \Delta x, \tag{10}$$

and the node function (5) in (6) and (8) will be positive semidefinite degenerate quadratic function

$$\psi_{\mathbf{i},j}(\mathbf{z}_{\mathbf{i},j} | Y_j, Y_{j+1}) = (\mathbf{z}_{\mathbf{i},j} - \mathbf{z}^0_{\mathbf{i},j})^T \mathbf{Q}^0_{\mathbf{i},j} (\mathbf{z}_{\mathbf{i},j} - \mathbf{z}^0_{\mathbf{i},j}) \tag{11}$$

where

$$\begin{gathered}
\mathbf{z}^0_{\mathbf{i},j} = \mathbf{z}^0_{\mathbf{i},j}(Y_j, Y_{j+1}) = \\
\frac{(y_{\mathbf{i},j} - y_{\mathbf{i},j+1})/\Delta x}{\big[\nabla_x y\big(\mathbf{i}\Delta x,\, (j+1)\Delta t\big)\big]^T \big[\nabla_x y\big(\mathbf{i}\Delta x,\, (j+1)\Delta t\big)\big]} \big[\nabla_x y\big(\mathbf{i}\Delta x,\, (j+1)\Delta t\big)\big], \\
\mathbf{Q}^0_{\mathbf{i},i} = \mathbf{Q}^0_{\mathbf{i},i}(Y_j, Y_{j+1}) = (\Delta x)^2 \big[\nabla_x y\big(\mathbf{i}\Delta x,\, (j+1)\Delta t\big)\big] \big[\nabla_x y\big(\mathbf{i}\Delta x,\, (j+1)\Delta t\big)\big]^T.
\end{gathered} \tag{12}$$

In this case, the penalty functions should be also taken in the quadratic form

$$\gamma_{\mathbf{i}',\mathbf{i}'',j}(\mathbf{z}_{\mathbf{i}',j}, \mathbf{z}_{\mathbf{i}'',j}) = (\mathbf{z}_{\mathbf{i}',j} - \mathbf{z}_{\mathbf{i}'',j})^T \mathbf{U}_{\mathbf{i}',\mathbf{i}'',j} (\mathbf{z}_{\mathbf{i}',j} - \mathbf{z}_{\mathbf{i}'',j}), \tag{13}$$

$$\gamma_{\mathbf{i},j,j+1}(\mathbf{z}_{\mathbf{i},j}, \mathbf{z}_{\mathbf{i},j+1}) = (\mathbf{z}_{\mathbf{i},j} - \mathbf{z}_{\mathbf{i},j+1})^T \mathbf{U}_{\mathbf{i},j,j+1} (\mathbf{z}_{\mathbf{i},j} - \mathbf{z}_{\mathbf{i},j+1}), \tag{14}$$

where $\mathbf{U}_{\mathbf{i}',\mathbf{i}'',j}$ and $\mathbf{U}_{\mathbf{i},j,j+1}$ are suitable positive definite matrices (2×2).

However, the approximation (10) is valid only for very small time steps $\Delta t = t_{j+1} - t_j$, what is hard to provide even if the time varying data set is obtained as result of numerical simulation, because the lack for memory space prevents from keeping the results of all the intervening steps when solving a system of differential equations. As a result, the node function (5) will no longer be quadratic (11), what will make the computational problem of minimizing the goal function much more difficult.

But if we replace the requirement to minimize the squared difference (5) of single values $y_{\mathbf{i},j}$ and $y_{\mathbf{i}+\mathbf{z}_{\mathbf{i},j},j+1}$ by that to minimize the squared norm of the difference between adjacent time slices in some vicinities of the corresponding points, the node functions will become much smoother functions of $\mathbf{z}_{\mathbf{i},j}$, and it will be possible to approximate them by quadratic functions

$$\psi_{\mathbf{i},j}(\mathbf{z}_{\mathbf{i},j}|Y_j,Y_{j+1}) = (\mathbf{z}_{\mathbf{i},j}-\mathbf{z}^0_{\mathbf{i},j})^T\mathbf{Q}^0_{\mathbf{i},j}(\mathbf{z}_{\mathbf{i},j}-\mathbf{z}^0_{\mathbf{i},j}) \cong \varphi_{\mathbf{i},j}(\mathbf{z}_{\mathbf{i},j}|Y_j,Y_{j+1}) = \sum_{\mathbf{m}\in\mathsf{M}}\big(y_{\mathbf{i}+\mathbf{m},j} - y_{\mathbf{i}+\mathbf{m}+\mathbf{z}_{\mathbf{i},j},j}\big)^2. \tag{15}$$

Here $\mathsf{M} = \big\{\mathbf{m}=(m_1,m_2):\ -M\le m_1\le M,\ -M\le m_2\le M\big\}$ is the elementary square fragment $(2M+1)\times(2M+1)$ around the reference point $\mathbf{i}$ and the search points $\mathbf{i}+\mathbf{z}'$ in which the current and the next time slices Y_j and Y_{j+1} are compared for tentative discrete shifts $\mathbf{z}'=(z^{(1)},z^{(2)})$ in a sufficiently large search area $z^{(1)}=-K,\dots,0,\dots,K$, $z^{(2)}=-K,\dots,0,\dots,K$. The resulting lattice function $\psi_{\mathbf{i},j}(\mathbf{z}'|Y_j,Y_{j+1})$ on the set of discrete points is to be approximated by a quadratic function $\varphi_{\mathbf{i},j}(\mathbf{z}'|Y_j,Y_{j+1})$ (15) whose range of definition is the two-dimensional real space as a whole.

We pass over the algorithm of evaluating parameters $\mathbf{z}^0_{\mathbf{i},j}$ and $\mathbf{Q}^0_{\mathbf{i},j}$ that determine quadratic node functions. The details can be found in [7, 8]. It is clear that the parameters will be real-valued. Vector $\mathbf{z}^0_{\mathbf{i},j}$ is the local estimate on the disparity value with eventual inter-pixel interpolation, and the nonnegative definite matrix $\mathbf{Q}^0_{\mathbf{i},j}$ carries the information on the reliability of this estimate in different directions in the image plane.

If point $\mathbf{i}$ is a salient point of the reference image and the similar peculiarity is present in the search one, it is very likely that $\mathbf{z}^0_{\mathbf{i},j}$ will be approximately equal to the spatial shift between them, and both positive eigenvalues of $\mathbf{Q}^0_{\mathbf{i},j}$ will be large in value, i.e. the second derivatives of the node function will be large in all directions from its minimum point, what means a very high reliability level of the local estimate on the disparity value.

In case $\mathbf{i}$ belongs to a ridge in the reference image and the analogous ridge is found also in the search image, it should be expected that $\mathbf{z}^0_{\mathbf{i},j}$ would show an occasional point of it, and the two eigenvalues of $\mathbf{Q}^0_{\mathbf{i},j}$ would be different. The eigenvector with the smaller eigenvalue will be directed along the ridge, so, the respective directional second derivative at the minimum point of the node function will be small, what means that there is no information on the disparity value in this direction. On the contrary, the larger eigenvalue of the orthogonal eigenvector will make the second derivative large in the transversal direction and indicate thereby a very high reliability level of the local estimate across the ridge.

Finally, if there are no informative peculiarities of the reference image in the vicinity of point $\mathbf{i}$, or the search image is noninformative in the area of admissible tentative shifts, both eigenvalues of $\mathbf{Q}^0_{\mathbf{i},j}$ will be small. In this case the small second derivatives of the node function in all directions from its occasional minimum point will indicate that the local estimate $\mathbf{z}^0_{\mathbf{i},j}$ does not deserve any reliance.

Within a single pair of adjacent time slices, the role of the edge functions $\gamma_{\mathbf{i}',\mathbf{i}'',j}(\mathbf{z}_{\mathbf{i}',j},\mathbf{z}_{\mathbf{i}'',j})$ in (6) is to smooth the local estimates on the neighboring goal variables $(\mathbf{z}_{\mathbf{i}',j},\mathbf{z}_{\mathbf{i}'',j})\in G_j$. The natural spatial symmetry suggests the identity of the edge functions associated with vertical and horizontal edges of the neighborhood lattice, so, the matrices in (13) should not differ from each other $\mathbf{U}_{\mathbf{i}',\mathbf{i}'',j}=\mathbf{U}'$. In the problem of apparent motion evaluation, because of the same spatial symmetry, it is hardly reasonable to take the matrix of the quadratic edge function in a more complicated form than diagonal matrix with the same value of all the diagonal elements $\mathbf{U}_{\mathbf{i}',\mathbf{i}'',j}=\mathbf{U}'=\mathrm{Diag}(u')$.

The temporal neighborhood relation between the slices differs in its nature from the spatial neighborhood within them, therefore, the edge functions $\gamma_{\mathbf{i},j,j+1}(\mathbf{z}_{\mathbf{i},j},\mathbf{z}_{\mathbf{i},j+1})$ in (8) should differ from $\gamma_{\mathbf{i}',\mathbf{i}'',j}(\mathbf{z}_{\mathbf{i}',j},\mathbf{z}_{\mathbf{i}'',j})$. But the same spatial symmetry determines the identity of all of them and the diagonal form of the identical matrices in (14) $\mathbf{U}_{\mathbf{i},j,j+1}=\mathbf{U}''=\mathrm{Diag}(u'')$.

Since both node and edge functions are taken in the quadratic form, the entire objective function of tracking (6) or (8) is also quadratic. If no smoothness constraints are imposed on the pairs of adjacent disparity maps Z_j and Z_{j+1} (6), each of $K-1$ sought-for arrays of spatial shifts $\hat{Z}_j(Y_j,Y_{j+1})$ is determined by an independent condition (7) which is equivalent to a system of N_1N_2 linear equations with the same number of two-dimensional vector variables, namely, as many as there are pixels in each time slice of the $2D+1$ time-varying data set being processed. If it is required to smooth the disparity maps, in addition, along the time axis (8), the number of equations and vector variables in the condition (9) that define $\hat{Z}(Y)=\big(\hat{Z}_j(Y_j,Y_{j+1}),\ j=1,\dots,K-1\big)$ increases still more drasticly, namely, up to N_1N_2K.

For such a huge number of variables, the intent to create a non-iterative procedure of finding the minimum point of a separable quadratic function supported by a lattice-like graph comes up against a fundamental barrier. Hence, the algorithm of finding the minimum point of the criterion (6) or (8) can be only of iterative type what is utterly undesirable for massive data sets.

One of the main results of the previous study [3, 4] is a noniterative optimization procedure for the particular case when the graph of the pair-wise adjacency of the data set elements has the form of a tree, i.e. has no cycles. The procedure is based on a recurrent decomposition of the initial optimization problem over all the node variables into a succession of partial problems each of which consists in optimization of a function of only one vector variable like Bellman functions in the classical dynamic programming.

But a tree is not yet the lattice, therefore, the basic optimization procedure cannot be immediately used for the processing of time-varying data sets. It is clear that there is no way to replace the lattice-like neighborhood graph by a tree-like one without loss in the ability to ensure the required smoothness of the secondary data field in all directions from each element of a data array ordered in space and time.

To avoid this obstacle, for finding the values of the hidden field at each single row of the data array, let it be conventionally the vertical row, it was proposed in [3, 4] to use a separate neighborhood tree which is defined, nevertheless, on the whole set of elements and has the same horizontal branches as the others (Fig. 4). The resulting generalized data processing procedure is aimed at finding the optimal values only for the goal variables at the stem

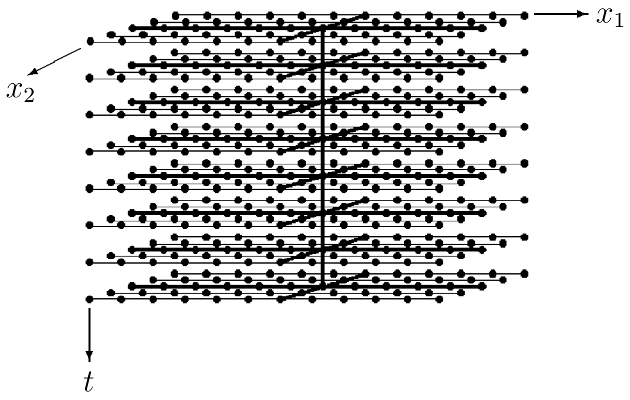

Figure 4: Tree-like adjacency graph of the partial objective function for evaluating the apparent motion vectors along the time axis at a single space point in $2D+1$ time-varying data sets.

nodes in each tree, and boils down to a combination of two usual dynamic programming procedures, each dealing with image rows of the data array, respectively, the horizontal and vertical ones.

We do not go here into details of the generalized data processing procedure that remains the same for many kinds of applications. The specificity of each particular data processing problem falls only on the way of extracting single units of the local information on the hidden variables immediately from the original data set and on the formalization of neighborhood constraints, i.e. on forming the quadratic node and edge functions, respectively, data-dependent (11) and model-based (13), (14). It is just this principle we applied in this work to the problem of apparent motion evaluation in fluid-dynamical time varying data sets.

The mathematical statement of this problem and the algorithm of matching adjacent pairs of time slices in a time varying data set essentially lean upon the assumption that the time step Δt is small. If the time-varying function $y(\mathbf{x}, t)$ is smooth enough, the matched slices $Y_j = Y(j\Delta t)$ and $Y_{j+1} = Y\big((j+1)\Delta t\big)$ will differ little from each other. As a result, it is possible to infer preliminary fuzzy estimates on the local apparent motion vectors in the form of quadratic node functions (11) immediately from picture fragments in some vicinities of candidate points. But if one considers a pair of time slices $Y(t')$ and $Y(t'')$ that are distant over quite a long time interval $(t''-t')$, the immediate similarity of elementary image fragments will gets lost, and the above described principle of matching will no longer be applicable. Nevertheless, it may be highly desired to follow the space trajectory of a salient point of the image flow while the respective pattern is sufficiently persistent.

The long-term tracking of salient peculiarities of a time-varying function can be done by composition of space transformations $\mathsf{R}^2 \to \mathsf{R}^2:\ \tilde{\mathbf{x}}(\mathbf{x}) = \mathbf{x} + \mathbf{z}(\mathbf{x}, t_j)$ defined by elementary apparent motion vectors estimated for successive sufficiently small steps of discrete time. Let $t' = j'\Delta t$ and $t'' = j''\Delta t$ be, respectively, the initial and terminal point of the time interval of interest, where $j'' = j' + k$, and $\mathbf{x}_{(j')}$ be the point in the initial slice $Y_{j'}$ we should like to track. For the first time step we have $\mathbf{x}_{(j'+1)} = \mathbf{x}_{(j')} + \mathbf{z}(\mathbf{x}_{(j')}, t_{j'})$, for the second one $\mathbf{x}_{(j'+2)} = \mathbf{x}_{(j'+1)} + \mathbf{z}(\mathbf{x}_{(j'+1)}, t_{j'+1})$, and so on, until we come to the terminal time moment $\mathbf{x}_{(j'')} = \mathbf{x}_{(j''-1)} + \mathbf{z}(\mathbf{x}_{(j''-1)}, t_{j''-1})$. The mapping $\mathbf{x}_{(j'')}(\mathbf{x}_{(j')})$ is just the long-term tracking we wish. To minimize, as possible, the inevitable accumulation of errors in the intervening vectors of apparent motion, they should be considered as real-valued ones $\mathbf{z}(\mathbf{x}_{(j)}, t_j) \in \mathsf{R}^2$ with inter-pixel interpolation of the next shift $\mathbf{z}(\mathbf{x}_{(j+1)}, t_{j+1}) = \mathbf{z}\big(\big(\mathbf{x}_{(j)} + \mathbf{z}(\mathbf{x}_{(j)}, t_j)\big),\ t_{j+1}\big)$ at an arbitrary point $\mathbf{x}_{(j+1)} = \mathbf{x}_{(j)} + \mathbf{z}(\mathbf{x}_{(j)}, t_j) \in \mathsf{R}^2$ from the apparent motion map $Z_{j+1} = \big(\mathbf{z}_{\mathbf{i},j+1} = \mathbf{z}(\mathbf{x}_{\mathbf{i}}, t_{j+1}),\ \mathbf{i} \in \mathsf{N}$ defined only for discrete space points $\mathbf{x}_{\mathbf{i}}$, $\mathbf{i} \in \mathsf{N}$.

5 Evaluation of apparent motion in simulated shock wave interaction with an elliptical bubble

In accordance with the above depicted approach, we evaluated the apparent motion in two constituents of a simulated $2D{+}1$ data flow. The original time-varying data set was obtained at the Department of Mechanical and Air-Space Engineering of Rutgers University [9] as numerical solution of a system of Euler differential equations (4) that represented the process of shock translating through space and hitting a prolate elliptical bubble of a heavier gas angled to the vertical. We analyzed physical pictures of density $\rho(\mathbf{x}, t)$ and vorticity $\omega(\mathbf{x}, t)$, the latter evaluated as rotation of the instantaneous velocity $\omega(\mathbf{x}, t) = \mathrm{Rot}\big(\mathbf{u}(\mathbf{x}, t)$. Each of the two time-varying data sets had the structure of a time series of 85 spatial distributions of the respective characteristic represented by its values at the nodes of a 700×640 pixels grid. Fig. 1 shows selected phases of both time-varying data sets.

A series of fragments of the estimated apparent motion maps is shown in Fig. 5 and 6. Each figure presents a pair of two immediately subsequent time slices of the respective physical picture. The dashes that emanate from the black markers forming a regular grid in the left (precedent) picture are exact representations of the estimated apparent motion vectors at the respective space points. The nodes of the deformed net in the right (immediately subsequent) picture are located just at the ends of the dashes and show the new positions of the picture elements marked by black markers at the left. So, the entire net gives a pictorial rendition of the instantaneous apparent motion as an elementary step of space warping within time interval Δt.

It is well seen that the form of the picture around each net node at the right is a practically perfect analog of that in the closest vicinity of the respective black marker at the left. It is just this analogy that has determined the apparent motion vectors at the space points where the picture exhibits some salient features. As to the vectors in noninfomative homogeneous areas, their values are formed, primarily, as result of interpolation or extrapolation from the estimates at the salient points.

Fig. 5 and 6 show how the same relatively persistent salient structure of the fluid flow manifests itself in two different characteristics. Comparison of the two estimates of apparent motion calculated from density and vorticity shows that they coincide quite well over the

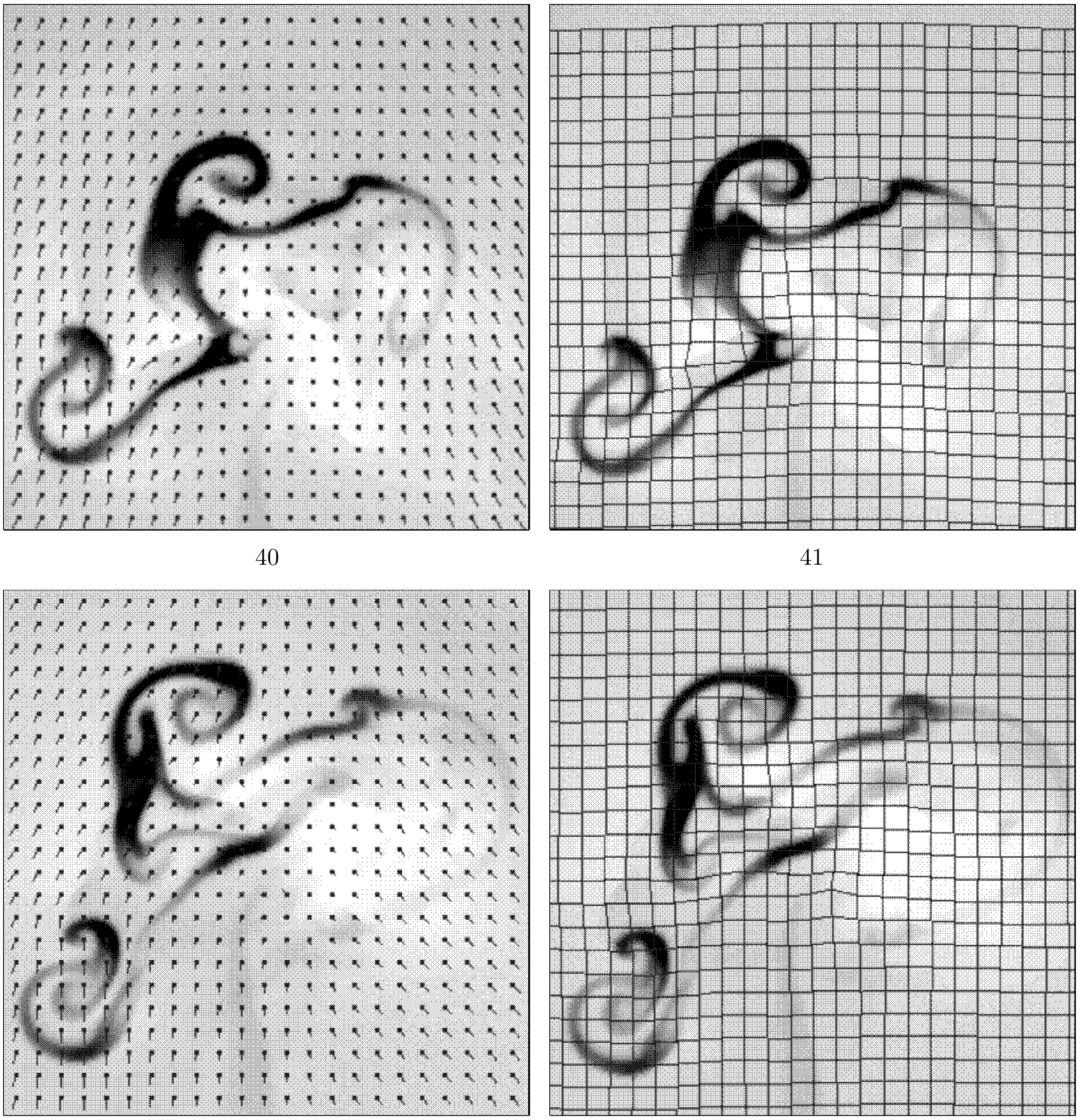

40 41

50 51

Figure 5: continued in the next page. Selected fragments of the apparent motion field estimated by image matching algorithm from pairs of adjacent time slices of simulated density (Fig. 1). In each of the pictures in this and the next page, vectors of the estimated apparent motion are shown in the precedent (left) time slice as dashes that emanate from bold markers forming an imaginary regular net and show the apparent motion of the respective element of the picture for one time step. The deformed net spanned in the next (right) time slice over the ends of the vectors shown at the left represents spatial warping of the precedent slice as result of apparent motion.

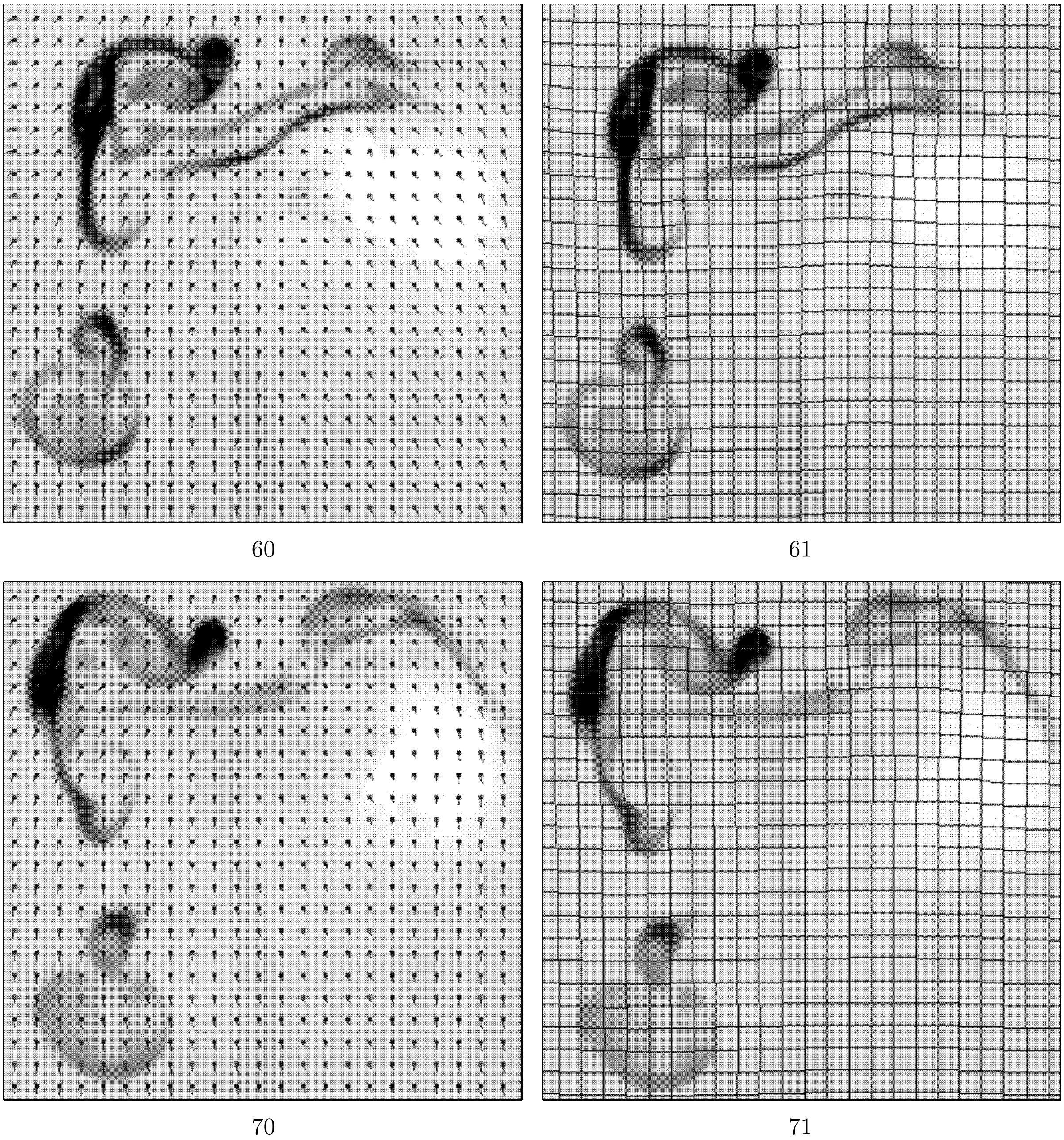

Figure 5: continuation from the previous page.

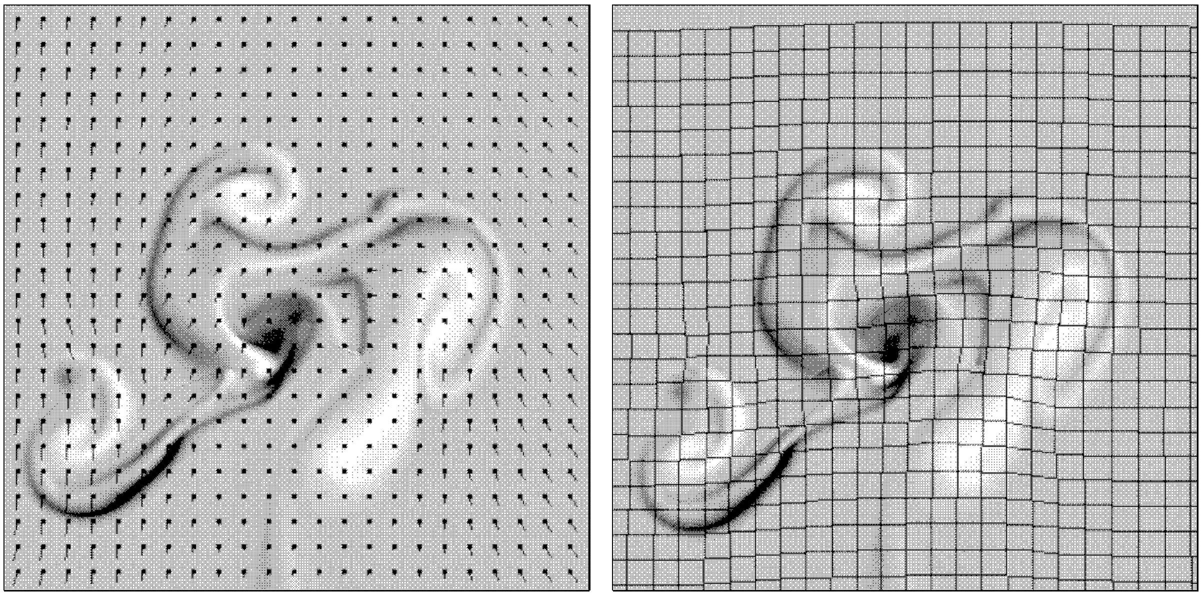

40 41

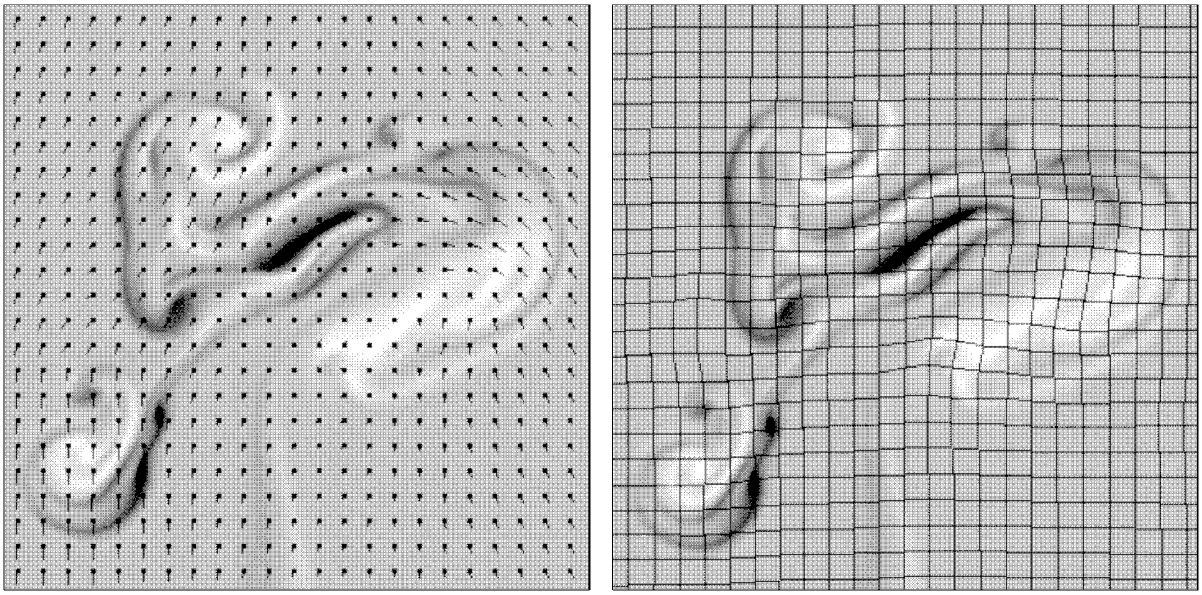

50 51

Figure 6: continued in the next page. Selected fragments of the apparent motion field estimated by image matching algorithm from pairs of adjacent time slices of simulated vorticity (Fig. 1). In each of the pictures in this and the next page, vectors of the estimated apparent motion are shown in the precedent (left) time slice as dashes that emanate from bold markers forming an imaginary regular net and show the apparent motion of the respective element of the picture for one time step. The deformed net spanned in the next (right) time slice over the ends of the vectors shown at the left represents spatial warping of the precedent slice as result of apparent motion.

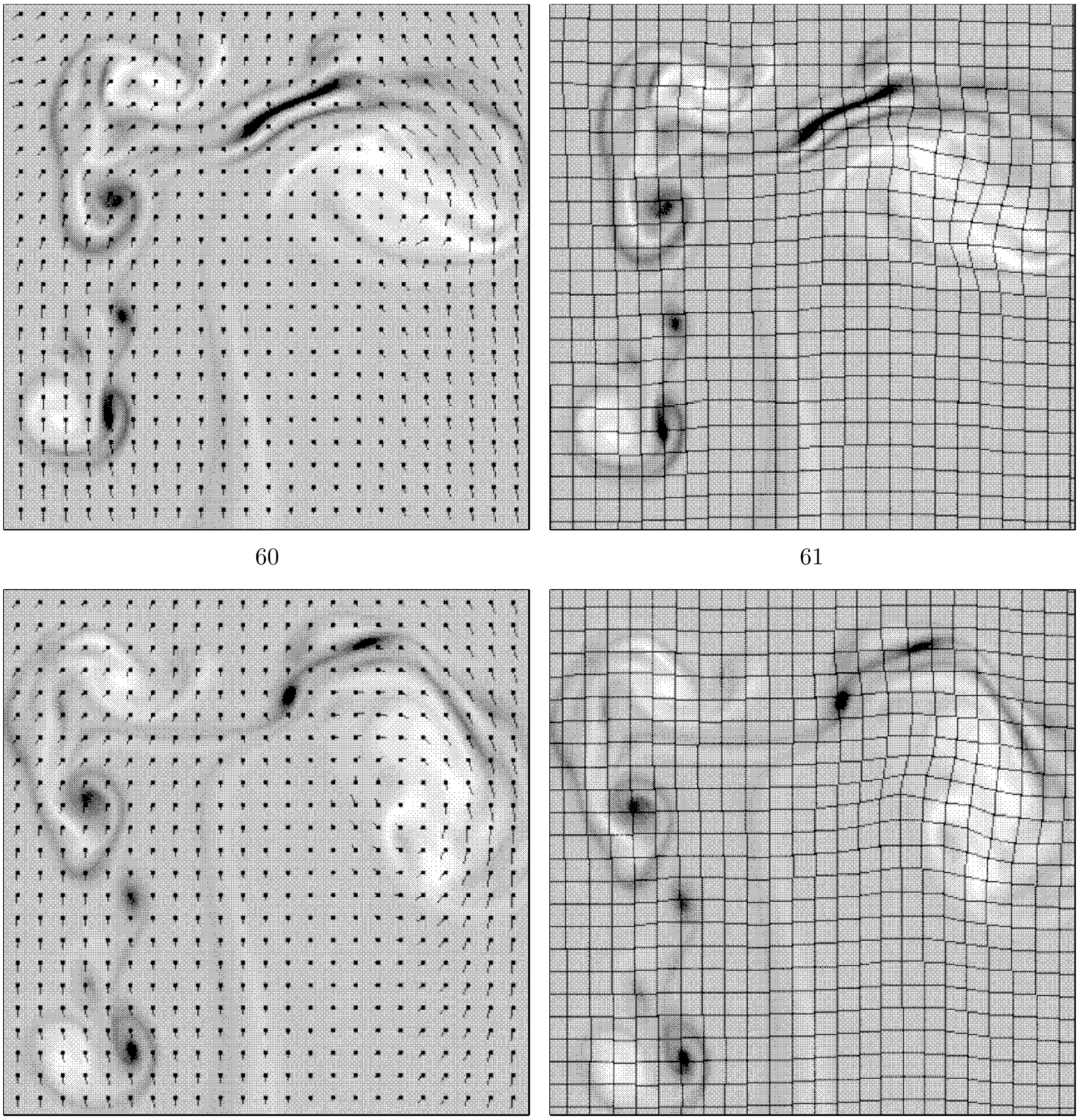

60 61

70 71

Figure 6: continuation from the previous page.

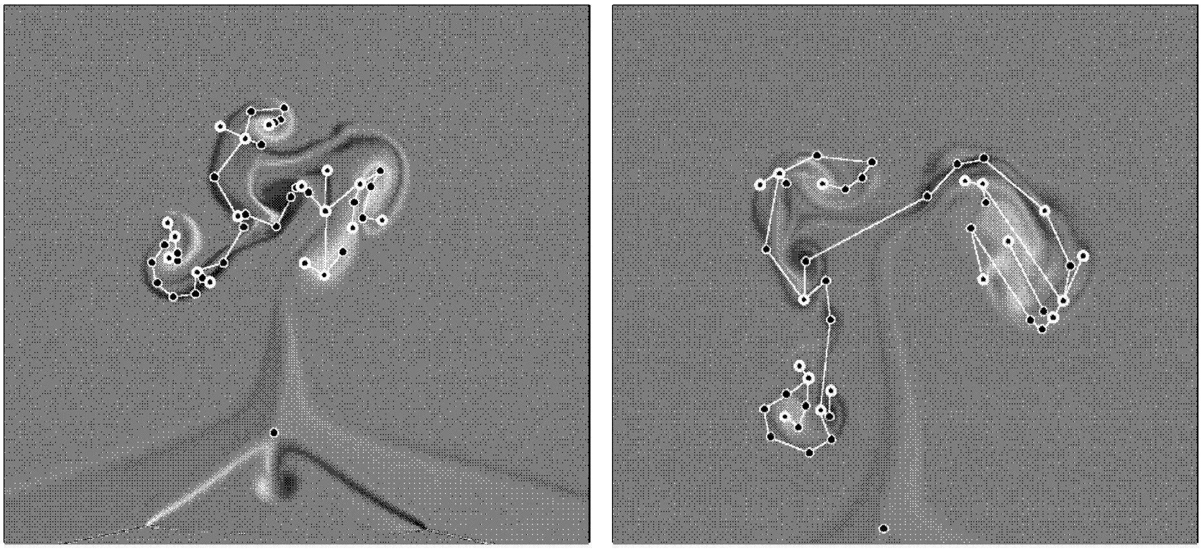

40 70

Figure 7: Result of pointwise long-term tracking in the time-varying picture of vorticity over 30 steps of discrete time. The markers in the left picture indicate the space points in the initial time slice that were tracked, and those in the right picture show their matches in the terminal slice. To facilitate visual recognition of the pairs of identical space points and the inheritance of respective coherent structures, the markers in the two pictures are combined by white lines into topologically similar figures. In addition, some of corresponding markers are highlighted with the same purpose.

basic part of the space fragment represented in the pictures except a pattern at the right. This pattern only faintly exhibits itself in density as a whitish spot of decreased values but is clearly pronounced in the vorticity. The major peculiarity of the pattern is the fact that it is relatively quickly rotating in the negative direction, that is, clockwise. This fact is especially conspicuous at the late phases of the process in the continuation of Fig. 6.

An example of long-term tracking in the time-varying picture of vorticity over 30 steps of discrete time is shown in Fig. 7. The markers in the left picture indicate the space points in the 40th time slice that were tracked, and those in the right picture show their matches in the 70th slice. To facilitate visual recognition of the pairs of identical space points and the inheritance of respective coherent structures, the markers in the two pictures are combined by white lines into topologically similar figures. In addition, some of corresponding markers are highlighted with the same purpose.

6 Differential equations of apparent motion

If the spatial step of the pixel grid N decreases infinitely $\Delta t \to 0$, the apparent motion maps $Z_j = (\mathbf{z}_{\mathbf{i},j},\, \mathbf{i} \in \mathsf{N})$ turn into vector-valued functions in the space of continuous pixel indices $Z_j = \big(\mathbf{z}_j(\mathbf{i}),\, \mathbf{i} \in \mathsf{R}^n\big)$. These functions are equivalent to the functions of space coordinates $\mathbf{x} = \mathbf{i}\Delta x$ that immediately indicate the shifts in terms of the original space $W_j = \big(\mathbf{w}(\mathbf{x},t) = \mathbf{z}_j(\mathbf{x}/\Delta x)\Delta x,\, \mathbf{x} \in \mathsf{X} = \mathsf{R}^n\big)$. On the other hand, if the time-varying function $y(\mathbf{x},t)$ is smooth both in time and space, an infinite diminution of the time step $\Delta t = t_{j+1} - t_j \to 0$ results in infinitely decreasing norms of apparent motion vectors $||\mathbf{w}(\mathbf{x},t_j)|| \to 0$, and, instead of full vectors, their derivatives with respect to time should be considered $\mathbf{v}(\mathbf{x},t) = \lim_{\Delta t \to 0} \big(\mathbf{w}(\mathbf{x},t)/\Delta t\big)$. In the limit, we shall have a time-varying function of apparent velocity $V = \big(\mathbf{v}(\mathbf{x},t),\, \mathbf{x} \in \mathsf{X} \subset \mathsf{R}^n,\, t \in \mathsf{T}\big)$ instead of the discrete succession of apparent motion maps.

With $\Delta t \to 0$, the approximate linear representation of a sufficiently smooth function (10) becomes exact

$$y\big(\mathbf{x} + \mathbf{v}(\mathbf{x},t)dt,\, t+dt\big) = y(\mathbf{x},t) + \big(\nabla_{\mathbf{x}} y(\mathbf{x},t)\big)^T \mathbf{v}(\mathbf{x},t)dt + \left(\frac{\partial}{\partial t} y(\mathbf{x},t)\right) dt =$$
$$y(\mathbf{x},t) + \left\{ \big(\nabla_{\mathbf{x}} y(\mathbf{x},t)\big)^T \mathbf{v}(\mathbf{x},t) + \left(\frac{\partial}{\partial t} y(\mathbf{x},t)\right) \right\} dt.$$

Thus, the local information on the sought-for value of the apparent velocity $\mathbf{v}(\mathbf{x},t)$ at the current point $\mathbf{x}$ is carried by the condition

$$\frac{y\big(\mathbf{x} + \mathbf{v}(\mathbf{x},t)dt,\, t+dt\big) - y(\mathbf{x},t)}{dt} = \left\{ \big(\nabla_{\mathbf{x}} y(\mathbf{x},t)\big)^T \mathbf{v}(\mathbf{x},t) + \left(\frac{\partial}{\partial t} y(\mathbf{x},t)\right) \right\} = 0. \qquad (16)$$

The equivalent form of the same condition will be the requirement that the respective quadratic function takes the minimum value:

$$\psi\big(\mathbf{v}(\mathbf{x},t);\, \mathbf{x},t\big) = \left\{ \big(\nabla_{\mathbf{x}} y(\mathbf{x},t)\big)^T \mathbf{v}(\mathbf{x},t) + \left(\frac{\partial}{\partial t} y(\mathbf{x},t)\right) \right\}^2 \to \min. \qquad (17)$$

It is clear that there always exists an $(n-1)$-dimensional subspace of $\mathbf{R}^n$ all points of which satisfy this condition. Moreover, the apparent velocity is not defined at stationary points of the time-varying function where $\nabla_{\mathbf{x}} y(\mathbf{x},t) = \mathbf{0}$.

On the other hand, the sought-for vector function $\mathbf{v}(\mathbf{x},t)$ must form a one-to-one mapping $\mathsf{R}^n \to \mathsf{R}^n\colon \tilde{\mathbf{x}} = \mathbf{x} + \mathbf{v}(\mathbf{x},t)\Delta t$ for sufficiently small time steps Δt. This property is guaranteed if $\mathbf{v}(\mathbf{x},t)$ is smooth in space, what, in its turn, is provided by the conditions $\partial^2 \mathbf{v}(\mathbf{x},t)/\partial x_k^2 < \infty$, $k = 1,\ldots,n$. One of the ways to ensure the smoothness, is to supplement (16) with additional requirements

$$\gamma'\left(\frac{\partial}{\partial x_k}\mathbf{v}(\mathbf{x},t)\right) = \left(\frac{\partial}{\partial x_k}\mathbf{v}(\mathbf{x},t)\right)^T \mathbf{U}' \left(\frac{\partial}{\partial x_k}\mathbf{v}(\mathbf{x},t)\right) \to \min, \quad k = 1,\ldots,n, \qquad (18)$$

where $\mathbf{U}'$ is an appropriate positive definite matrix $(n \times n)$. A compromise between these conditions and (16) is provided by the functional

$$J\big(V(t), t\big) = \int\limits_{\mathsf{X}} \left\{ \psi\big(\mathbf{v}(\mathbf{x}, t); \mathbf{x}, t\big) + \sum_{k=1}^{n} \gamma'_k \left(\frac{\partial}{\partial x_k} \mathbf{v}(\mathbf{x}, t) \right) \right\} d\mathbf{x} \to \min \tag{19}$$

which is a continuous analog of the discrete functional (16). The vector function $V(t) = \big(\mathbf{v}(\mathbf{x}, t),\, \mathbf{x} \in \mathsf{X} \subset \mathsf{R}^n\big)$ that delivers the minimum value to this functional should be considered as the sought-for apparent velocity field at time moment t. Since the functional depends on time, it determines all the apparent velocity fields, independently of each other, for all the time moments in the interval under consideration $t \in \mathsf{T} = (t^{\min}, t^{\max})$.

The optimization problems for different time moments will no longer be independent, if we impose quadratic smoothness constraints, in addition to space coordinates (18), also upon the first derivative of $\mathbf{v}(\mathbf{x}, t)$ with respect to time

$$\gamma'' \left(\frac{\partial}{\partial t} \mathbf{v}(\mathbf{x}, t) \right) = \left(\frac{\partial}{\partial t} \mathbf{v}(\mathbf{x}, t) \right)^T \mathbf{U}'' \left(\frac{\partial}{\partial t} \mathbf{v}(\mathbf{x}, t) \right) \to \min, \tag{20}$$

where positive definite matrix $\mathbf{U}''$ differs, in the general case, from matrix $\mathbf{U}'$ in (18). In this case, to find the time-varying apparent velocity $V = \big(\mathbf{v}(\mathbf{x}, t),\, \mathbf{x} \in \mathsf{X} \subset \mathsf{R}^n,\, t \in \mathsf{T}\big)$, it is required to solve the optimization problem with the combined functional

$$J(V) = \int\limits_{\mathsf{T}} \int\limits_{\mathsf{X}} \left\{ \psi\big(\mathbf{v}(\mathbf{x}, t); \mathbf{x}, t\big) + \sum_{k=1}^{n} \gamma'_k \left(\frac{\partial}{\partial x_k} \mathbf{v}(\mathbf{x}, t) \right) + \left(\frac{\partial}{\partial t} \mathbf{v}(\mathbf{x}, t) \right) \right\} d\mathbf{x}\, dt \to \min \tag{21}$$

which is analogous to the discrete version (8). It is enough to consider only this problem, because (19) follows from it if $\mathbf{U}'' = \mathbf{0}$.

The optimization problem (21) is the classical problem of the calculus of variations, and its solution is determined by the system of Euler differential equations. To simplify the mathematical treatment and clarify the structure of the solution, let us represent the local criterion (17) in a canonical form:

$$\psi\big(\mathbf{v}(\mathbf{x}, t); \mathbf{x}, t\big) = \big(\mathbf{v}(\mathbf{x}, t) - \mathbf{v}^0(\mathbf{x}, t)\big)^T \mathbf{Q}^0(\mathbf{x}, t) \big(\mathbf{v}(\mathbf{x}, t) - \mathbf{v}^0(\mathbf{x}, t)\big). \tag{22}$$

To make sure that

$$\mathbf{Q}^0(\mathbf{x}, t) = \big(\nabla_{\mathbf{x}} y(\mathbf{x}, t)\big)\big(\nabla_{\mathbf{x}} y(\mathbf{x}, t)\big)^T \tag{23}$$

is the Hessian matrix of this degenerate quadratic form, it is enough to square the expression in the braces in (17). As to the conventional minimum point $\mathbf{v}^0(\mathbf{x}, t)$, any vector is suited that satisfies the equality (16). It is reasonable to take the shortest of them $\mathbf{v}^T \mathbf{v} \to \min$, then we shall have

$$\mathbf{v}^0(\mathbf{x}, t) = -\nabla_{\mathbf{x}} y(\mathbf{x}, t) \frac{\dfrac{\partial}{\partial t} y(\mathbf{x}, t)}{\big(\nabla_{\mathbf{x}} y(\mathbf{x}, t)\big)^T \big(\nabla_{\mathbf{x}} y(\mathbf{x}, t)\big)}. \tag{24}$$

For the criterion (21), we have the following system of Euler equations:

$$\begin{cases} \displaystyle\sum_{k=1}^{n} \frac{\partial}{\partial x_k}\left(\frac{\partial \gamma'}{\partial(\partial v_1/\partial x_k)}\right) + \frac{\partial}{\partial t}\left(\frac{\partial \gamma''}{\partial(\partial v_1/\partial t)}\right) - \frac{\partial \psi}{\partial v_1} = 0, \\ \qquad\qquad\qquad\qquad \cdot \quad \cdot \quad \cdot \\ \displaystyle\sum_{k=1}^{n} \frac{\partial}{\partial x_k}\left(\frac{\partial \gamma'}{\partial(\partial v_n/\partial x_k)}\right) + \frac{\partial}{\partial t}\left(\frac{\partial \gamma''}{\partial(\partial v_n/\partial t)}\right) - \frac{\partial \psi}{\partial v_n} = 0, \end{cases}$$

or, in the vector form,

$$\sum_{k=1}^{n} \frac{\partial}{\partial x_k}\left[\nabla_{\partial \mathbf{v}/\partial x_k}\gamma'\left(\frac{\partial}{\partial x_k}\mathbf{v}(\mathbf{x},t)\right)\right] + \frac{\partial}{\partial t}\left[\nabla_{\partial \mathbf{v}/\partial t}\gamma''\left(\frac{\partial}{\partial x_k}\mathbf{v}(\mathbf{x},t)\right)\right] - \nabla_{\mathbf{v}}\psi\big(\mathbf{v}(\mathbf{x},t);\, \mathbf{x},t\big) = \mathbf{0}.$$

Rewriting this system in terms of (18), (20) and (22), we obtain the final system of partial differential equations that determine the sought-for apparent velocity $\mathbf{v}(\mathbf{x},t)$

$$\mathbf{U}'\sum_{k=1}^{n} \frac{\partial^2}{\partial x_k^2}\mathbf{v}(\mathbf{x},t) + \mathbf{U}''\frac{\partial^2}{\partial t^2}\mathbf{v}(\mathbf{x},t) - \mathbf{Q}^0\big(\mathbf{v}(\mathbf{x},t) - \mathbf{v}^0(\mathbf{x},t)\big) = \mathbf{0} \tag{25}$$

where the time-varying function $y(\mathbf{x},t)$ to be analyzed occurs through the matrix function $\mathbf{Q}^0(\mathbf{x},t)$ (23) and the vector function $\mathbf{v}^0(\mathbf{x},t)$ (24).

It should be emphasized that function $\mathbf{v}^0(\mathbf{x},t)$ is no solution of this system, because matrix $\mathbf{Q}^0(\mathbf{x},t)$ is degenerate at each point $(\mathbf{x},t)$, and even very small positive definite penalty matrices $\mathbf{U}'$ and $\mathbf{U}''$ may lead the actual solution $\mathbf{v}(\mathbf{x},t)$ far away of $\mathbf{v}^0(\mathbf{x},t)$.

These matrices are to be preset by the researcher as parameters that determine the desired smoothing degree for different components of apparent velocity in different directions in space and time. In particular, if no smoothing along the time axis is desired, the latter matrix should be put zero $\mathbf{U}'' = \mathbf{0}$, and system (25) falls into a continuous set of independent systems each of which determines the apparent velocity field for a specific time value.

As the simplest choice, it is expedient to take the penalty matrices in the diagonal form $\mathbf{U}' = u'\mathbf{I}$ and $\mathbf{U}'' = u''\mathbf{I}$, where $u' > 0$, $u'' > 0$, and $\mathbf{I}$ is identity matrix. In this case, the differential equation (25) can be rewritten in a simpler form:

$$u'\sum_{k=1}^{n} \frac{\partial^2}{\partial x_k^2}\mathbf{v}(\mathbf{x},t) + u''\frac{\partial^2}{\partial t^2}\mathbf{v}(\mathbf{x},t) - \mathbf{Q}^0(\mathbf{x},t)\big(\mathbf{v}(\mathbf{x},t) - \mathbf{v}^0(\mathbf{x},t)\big) = \mathbf{0} \tag{26}$$

where $u'' = 0$ if smoothing in time is not required.

In the problems of fluid dynamics, the time-varying function $y(\mathbf{x},t)$ to be analyzed is defined, as a rule, by a system of partial differential equations along with some other functions forming jointly the generalized state variable of the respective dynamic system. In this case, equation system (24) or (25) can be incorporated to the main system. Then, the resulting extended system of partial differential equations will determine the apparent velocity in addition to the actual one. The additional equations will not impede the process of numerical solving the main system, because it is linear with respect to the sought-for function $v(\mathbf{x},t)$, and the analyzed function $y(\mathbf{x},t)$, which nonlinearly occurs is the equation, is completely defined by the main system.

7 Conclusions

The idea of evaluating apparent motion in flows of spatially disributed data is no radically new one, it is only a specification and generalization of the thresholding technique proposed in the preceding studies as a means for tracking regions of interest in spatial time-varying data sets. What is new here is the suggestion to track in time not the entire amorphous objects but single space point with the intent to use the resulting field of apparent streamlines for tracking any regions that may be of interest in the context of a particular investigation. But it is just this point that invites further research because it raises more questions than we have answered here.

It is the typical situation that an amorphous pattern of the image flow moves in space as a whole, but, at the same time, it consists of several lesser patterns that are moving, it their turn, inside it. For instance, a translating and rotating structure is clearly seen in the right parts of vorticity pictures in Fig. 6.

Since the same point of space participates, as a rule, in several apparent motions that sum up into a resulting composite one, it may be important to distinguish between several hierarchical levels of apparent motion. What we evaluate in the form of the time-varying field of apparent velocities is the lowest level of this hierarchy that represents the overall rate of more elementary apparent motions.

There is an analogy between superposition of motions in the classical mechanics and that of apparent motions, but this analogy is far of full identity.

On the one hand, the usual linear composition of velocity vectors is completely applicable to the apparent motion. In particular, just as any vector field, the time-varying field of apparent velocities can be uniquely decomposed into the irrotational (potential) and the divergence-free (purely vortical) component. The divergence and vorticity of an apparent velocity field are new time-varying functions of space coordinates that, in their turn, may be analyzed by the same technique and characterized, on a higher level of hierarchy, by secondary apparent velocities.

It should be marked that even a divergence-free fluid flow without sources and drains may produce an apparent velocity field with non-zero divergence if an amorphous structure increases or decreases in size.

On the other hand, elementary apparent motions may superimpose in a less straightforward manner than usual mechanical ones. For instance, two stones thrown in quiet water produce waves on its surface that will manifest themselves as a composite apparent motion in the time-varying water level forming a function of two space coordinates. But the apparent velocity field computed immediately from the original time-varying function will be a scrappy picture changing in time in a complicated manner. Nevertheless, it is a nonlinear composition of two irrotational time-varying vector fields which are to be restored by relevant methods with respect to the mechanism of wave superposition.

The idea of pointwise apparent motion rests on the isosurface-based approach to tracking coherent structures in time-varying data sets and, so, implies the motion of isosurfaces of the respective time-varying function. The role of the variational principle in the evaluation of apparent motion, as it was originally conceived in this work, boiled down to elimination of the ambiguity which inevitably arises when trying to represent the motion of an isosurface as that formed by the multitude of pointwise ones. It is just this mission that is performed by the variational principle in forming differential equations of apparent motion for infinitesimally small time steps. But to simplify the search of identical space points in the case of macroscopic time steps, we were forced to resort to replacing single space points by their sufficiently large vicinities. As a result, the new apparent position of the current point is sought-for not from the principle of conservation of value but from that of retention of form. Although it is, to be strict, not the same, such a principle may be not less reasonable, because it allows for tracking persistent patterns of decreasing magnitude. Otherwise, such patterns would fall under the threshold and get lost.

Finally, the proposed technique of apparent motion evaluation can be applied not only to the time-varying function itself but also to the result of some preprocessing of it. For instance, it may be of interest to analyze spatial spectral constituents of the original function and distinguish, thereby, between apparent motion in high-frequency and low-frequency band.

8 Acknowledgements

This work was done in the period June 23 - August 13, 1999, when Dr. Vadim Mottl and Dr. Alexander Blinov visited Rutgers University on the invitation of Dr. Norman Zabusky. These co-authors are grateful to him for the possibility to get acquainted, if only perfunctorily, with the fascinating world of fluid dynamics and time-varying data visualization.

All the authors are grateful to Dr. Alexei Kotelnikov and Dr. Yuriy Gulak for numerous helpful discussions that contributed very much to the final contents of this work.

References

[1] Samtaney, R., Silver, D., Zabusky, N., Cao, J. Visualizing features and tracking their evolution. *IEEE Computer*, 27(7): 20-27, July 1994.

[2] Wang, X. *Visualization and tracking features in 3D time-varying datasets.* Ph.D. Thesis. Rutgers University, 1998.

[3] Muchnik, I., Mottl, V. *Optimization Algorithms for Separable Functions with Tree-Like Adjacency of Variables and their Application to the Analysis of Massive Data Sets.* DIMACS Technical Report 97-16, April 1997. Center for Discrete Mathematics and Theoretical Computer Science. Rutgers University, the State University of New Jersey.

[4] Muchnik, I., Mottl, V. *Bellman Functions on Trees for Segmentation, Generalized Smoothing, Matching and Multi-Alignment in Massive Data Sets.* DIMACS Technical Report 98-15, April 1998. Center for Discrete Mathematics and Theoretical Computer Science. Rutgers University, the State University of New Jersey.

[5] Bitz, F., Zabusky, N. David. "Visiometrics": Visualizing and quantifying evolving amorphous objects. *Comput. Phys.*, Nov/Dec: 603-14.

[6] Zabusky, N. Vortex paradigm for accelerated inhomogeneous flows: Visiometrics for the Rayleigh-Taylor and Richtmyer-Meshkov enviroments. *Annu. Rev. Fluid Mech.*, 1999, 31: 495-536.

[7] Mottl, V.V., Kopylov, A.V. Algorithms for matching images with raster distortions. *Pattern Recognition and Image Analysis. Advances in Mathematical Theory and Applications*, 1996, Vol. 6, No. 4.

[8] Mottl, V.V., Blinov, A.B., Kopylov, A.V., Kostin, A.A. Optimization techniques on pixel neighborhood graphs for image processing. *Graph Based Representations in Pattern Recognition.* Computing, Supplement 12. Springer, 1998. Pp. 135-145.

[9] Zabusky, N., Ray, J. Circulation deposition and emergence of vortex clusters from shock-bubble interaction. *Proceedings of the 2nd International Workshop on Laboratory Astrophysics with Intense Lasers*, 1998.